

## THE $L_X - T$ RELATION AND TEMPERATURE FUNCTION FOR NEARBY CLUSTERS REVISITED

MAXIM MARKEVITCH<sup>1</sup>

Harvard-Smithsonian Center for Astrophysics, 60 Garden St., Cambridge, MA 02138; maxim@head-cfa.harvard.edu

*ApJ in press, 1998 September 1*

### ABSTRACT

The X-ray luminosity-temperature relation for nearby  $T \simeq 3.5 - 10$  keV clusters is rederived using new *ASCA* temperatures (Markevitch et al. 1998a) and *ROSAT* luminosities. Both quantities are derived by directly excluding the cooling flow regions. This correction results in a greatly reduced scatter in the  $L_X - T$  relation; cooling flow clusters are similar to others outside the small cooling flow regions. For a fit of the form  $L_{\text{bol}} \propto T^\alpha$ , we obtain  $\alpha = 2.64 \pm 0.27$  (90%) and a residual rms scatter in  $\log L_{\text{bol}}$  of 0.10. The derived relation can be directly compared to theoretical predictions that do not include radiative cooling. It also provides an accurate reference point for future evolution searches and comparison to cooler clusters.

The new temperatures and  $L_X - T$  relation together with a newly selected cluster sample are used to update the temperature function at  $z \sim 0.05$ . The resulting function is generally higher and flatter than, although within the errors of, the previous estimates by Edge et al. (1990) and Henry & Arnaud (1991, as rederived by Eke et al. 1996). For a qualitative estimate of constraints that the new data place on the density fluctuation spectrum, we apply the Press-Schechter formalism for  $\Omega_0 = 1$  and 0.3. For  $\Omega_0 = 1$ , assuming cluster isothermality, the temperature function implies  $\sigma_8 = 0.55 \pm 0.03$ , while taking into account the observed cluster temperature profiles,  $\sigma_8 = 0.51 \pm 0.03$ , consistent with the previously derived range. The dependence of  $\sigma_8$  on  $\Omega_0$  differs from earlier findings, because of our treatment of the slope of the fluctuation spectrum  $n$  as a free parameter. For the considered values of  $\Omega_0$ ,  $n = -(2.0 - 2.3) \pm 0.3$ , somewhat steeper than derived from the earlier temperature function data, in agreement with the local slope of the galaxy fluctuation spectrum from the APM survey (Baugh & Gaztañaga 1996), and significantly steeper than the standard CDM prediction.

*Subject headings:* Cooling flows — cosmology — galaxies: clusters: individual — intergalactic medium —  
X-rays: galaxies

### 1. INTRODUCTION

Clusters exhibit a correlation between their X-ray luminosity and temperature, approximately  $L_{\text{bol}} \propto T^3$  (Mushotzky 1984; Edge & Stewart 1991; David et al. 1993; Fukazawa 1997). However, models of cluster evolution that assume no segregation of dark and gaseous matter predict  $L_{\text{bol}} \propto T^2$  (e.g., Kaiser 1986; Navarro, Frenk, & White 1995). This discrepancy suggests that the gas is distributed and evolves differently from the dark matter. One of the proposed reasons for this difference is preheating of the intracluster gas by an agent other than gravity, such as supernovae, at some high redshift (Kaiser 1991; Evrard & Henry 1991). Significant energy injection to the gas should have been made at the time of its enrichment with heavy elements (e.g., David, Forman, & Jones 1991; Loewenstein & Mushotzky 1996), although neither the amount nor the epoch of such injection is certain. Models that allow preheating succeed in approximately reproducing the observed  $L_X - T$  slope (e.g., Navarro et al. 1995). If the gas was preheated and later subjected to merger shocks, cooler clusters and groups are expected to have a steeper  $L_X - T$  dependence than hot clusters (e.g., Cavaliere et al. 1997), for which there is some observational indication (Ponman et al. 1996). Also, preheating should make the redshift evolution of the  $L_X - T$  relation slower or absent (Evrard & Henry 1991). Indeed, observations exclude any dramatic evolution out to  $z \simeq 0.3 - 0.5$  (Tsuru et al. 1996; Mushotzky & Scharf 1997), although this may also be expected in low  $\Omega_0$  models without preheating (e.g., White & Rees 1978; Eke, Navarro, & Frenk 1998).

The previously reported  $L_X - T$  relation at both low and high redshifts exhibits a large scatter which precludes accurate determination of its exact shape and evolution. Fabian et al. (1994) noted that the scatter is mostly due to the strong cooling flow clusters. Cooling flow regions, present in more than a half of all low-redshift clusters (e.g., Edge, Stewart, & Fabian 1992), are governed by a different physics than the bulk of the cluster gas, while in extreme cases emitting most of the X-ray luminosity and strongly biasing the wide-beam temperature measurements (e.g., Allen 1998). Cluster evolution models mentioned above predict global properties of the cluster gas and generally ignore the presence of cooling flows, thus it is not obvious that their predictions can be meaningfully compared to the observations. In principle, radiative cooling can be included in the models, but it appears that with greater certainty its effects can be separated in the data, which we attempt in this paper.

The  $L_X - T$  relation is a necessary tool for derivation of the cluster temperature function using a flux-limited sample. For low-redshift clusters, this function was previously obtained by Edge et al. (1990, hereafter E90) and Henry & Arnaud (1991, hereafter HA; see correction in Eke, Cole, & Frenk 1996). Since the gas temperature is linked to the total cluster mass, the temperature function provides information on the spectrum of the cosmological density fluctuations (e.g., HA), as well as on  $\Omega_0$  with additional data from higher  $z$  (e.g., Henry 1997 and references therein). The least certain link in this line of argument is the conversion from the observed temperature to the cluster mass, which has usually been made assuming cluster isothermality or near-isothermality. However, recent *ASCA* re-

<sup>1</sup> Also Space Research Institute, Russian Academy of Sciences

sults (e.g., Markevitch et al. 1998a, hereafter M98) indicate considerable spatial temperature variations which affect the temperature-mass relation. In addition, the temperature function itself is affected by cooling flows via sample selection, individual temperature errors, and the  $L_X - T$  relation. All these effects should be corrected for an accurate comparison with theoretical models.

In this paper, we use the new *ASCA* cluster mean temperatures obtained by directly excluding cooling flow regions (M98) and similarly corrected luminosities for a cluster sample selected from the new *ROSAT* All-Sky dataset. With these data, we rederive the low-redshift  $L_X - T$  relation and the temperature function which can be directly compared to theoretical predictions as well as to the oncoming high quality data from higher redshifts. An accurate comparison with models is best performed by detailed simulations and is left for future work; for a qualitative estimate of the constraints that the new data place on the density fluctuation spectrum, we apply a Press-Schechter formalism for  $\Omega_0 = 1$  and 0.3. We use  $H_0 = 100 h \text{ km s}^{-1} \text{ Mpc}^{-1}$ ; confidence intervals are one-parameter 90% unless stated otherwise.

## 2. THE SAMPLE

The sample is selected from the *ROSAT* All-Sky Survey (RASS) Abell cluster list (Ebeling et al. 1996) plus three known bright non-Abell clusters, with  $0.04 \leq z \leq 0.09$  and  $f(0.1 - 2.4 \text{ keV}) > 2 \times 10^{-11} \text{ erg s}^{-1} \text{ cm}^{-2}$ . Because the RASS fluxes have some uncertainty, pointed *ROSAT* PSPC or *Einstein* IPC observations of all clusters with the RASS fluxes greater than 3/4 of the above limit were analyzed to derive accurate fluxes and luminosities. The rederived fluxes correspond to the aperture of  $r = 1 h^{-1} \text{ Mpc}$  (which includes practically all the flux) centered on the X-ray emission centroid, and exclude all contaminating sources. Below, these fluxes and corresponding luminosities are referred to as “total”.

Cooling flows were excised from fluxes and luminosities already at the sample selection step, for consistency with the analysis below. A  $50 h^{-1} \text{ kpc}$  radius contains most of the cooling flow emission in nonextreme cooling flow clusters such as those in our sample. Therefore, to do the excision in a uniform manner, for all clusters, regions of  $50 h^{-1} \text{ kpc}$  radius centered on the main brightness peak were masked, and the resulting fluxes and luminosities were multiplied by 1.06 to account for the flux inside the masked region assuming an average  $\beta$ -model for the cluster X-ray brightness,  $S_X \propto (1 + r^2/a_x^2)^{-3\beta+1/2}$  with  $a_x = 125 h^{-1} \text{ kpc}$  and  $\beta = 0.6$  (Jones & Forman 1984). We refer to these fluxes and luminosities as “corrected”. For clusters with strong cooling flows (e.g., A478, A780, A2597), this correction significantly reduces the flux; for clusters lacking cooling flows, the flux is (by design) practically unchanged. Note that this correction procedure is only approximate and is not intended to result in the exact removal of the cooling flow contribution, which obviously would require a detailed modeling. However, its simplicity and model-independence enables a straightforward comparison to the current simulations that lack resolution to reproduce cluster high-density regions.

Use of more accurate fluxes from pointed observations has resulted in adding A3391 and removing A3532 from the original sample, while excision of cooling flows has resulted in removing A133 and A2597 (with the latter still being used for the  $L_X - T$  relation, as it has been already analyzed). Because cooling flows only increase the total flux, with high certainty no clusters from the Ebeling et al. (1996) list that satisfy our crite-

ria were missed. Table 1 lists the final full cluster sample with total and corrected luminosities and corrected fluxes. Accuracy of the measured fluxes and luminosities is around 5% due to the uncertainties in *ROSAT* calibration, background, Galactic absorption, etc.

TABLE 1  
FULL CLUSTER SAMPLE

Name	$z$	$T_{\text{fit}}^a$	$T_{\text{corr}}^a$	$L_{X\text{tot}}^b$	$L_X^c$	$L_{\text{bol}}^c$	$f_X^c$
A85	0.052	$6.1 \pm 0.2$	$6.9 \pm 0.4$	2.22	1.90	4.54	6.54
A119	0.044	$5.8 \pm 0.6$	$5.6 \pm 0.3$	0.85	0.88	1.85	4.14
A399	0.072	$7.4 \pm 0.7$	$7.0 \pm 0.4$	1.66	1.71	4.12	3.07
A401	0.074	$8.3 \pm 0.5$	$8.0 \pm 0.4$	2.90	2.87	7.49	4.93
A478	0.088	$7.1 \pm 0.4$	$8.4^{+0.8}_{-1.4}$	4.15	3.21	8.62	3.87
A644*	0.071	$7.1 \pm 0.6$	$7.9 \pm 0.8$	2.07	1.87	4.83	3.44
A754	0.054	$9.0 \pm 0.5$	$9.5^{+0.7}_{-0.4}$	2.19	2.22	6.44	7.07
A780	0.057	$3.8 \pm 0.2$	$4.3 \pm 0.4$	1.68	1.17	2.12	3.40
A1644	0.048	$4.7 \pm 0.8$ d	5.0 e	0.94	0.93	...	3.79
A1650	0.085	$5.6 \pm 0.6$	$6.7 \pm 0.8$	1.88	1.85	4.32	2.39
A1651	0.085	$6.3 \pm 0.5$	$6.1 \pm 0.4$	1.97	1.80	4.07	2.35
A1736	0.046	$3.5 \pm 0.4$	$3.5 \pm 0.4$	0.50	0.50	0.83	2.18
A1795	0.062	$6.0 \pm 0.3$	$7.8 \pm 1.0$	2.60	1.98	5.09	4.78
A2029	0.077	$8.7 \pm 0.3$	$9.1 \pm 1.0$	4.28	3.38	9.40	5.39
A2065	0.072	$5.4 \pm 0.3$	$5.5 \pm 0.4$	1.29	1.27	2.66	2.24
A2142	0.089	$8.8 \pm 0.6$	$9.7^{+1.5}_{-1.1}$	5.22	4.83	14.19	5.68
A2256	0.058	$7.5 \pm 0.4$	$6.6 \pm 0.4$	2.15	2.18	5.06	6.01
A2319*	0.056	$9.2 \pm 0.7$	$8.8 \pm 0.5$	3.67	3.64	10.06	11.09
A2589	0.042	$3.7^{+2.2}_{-1.2}$ d	3.5 e	0.51	0.44	...	2.38
A2597†	0.085	$3.6 \pm 0.2$	$4.4^{+0.4}_{-0.7}$	1.73	0.98	1.81	1.26
A2657	0.040	$3.7 \pm 0.3$	$3.7 \pm 0.3$	0.47	0.42	0.71	2.44
A3112	0.070	$4.7 \pm 0.4$	$5.3^{+0.7}_{-1.0}$	1.64	1.15	2.34	2.16
A3158	0.059	$5.5 \pm 0.6$ d	6.0 e	1.41	1.38	...	3.68
A3266	0.055	$7.7 \pm 0.8$	$8.0 \pm 0.5$	1.82	1.83	4.78	5.76
A3376	0.046	$4.3 \pm 0.6$	$4.0 \pm 0.4$	0.56	0.57	0.99	2.44
A3391	0.054	$5.7 \pm 0.7$	$5.4 \pm 0.6$	0.74	0.74	1.52	2.39
A3395	0.050	$4.8 \pm 0.4$	$5.0 \pm 0.3$	0.79	0.81	1.60	3.05
A3558	0.048	$5.5 \pm 0.3$	$5.5 \pm 0.4$	1.74	1.68	3.51	6.89
A3562	0.050	$3.8 \pm 0.9$ d	4.8 e	0.90	0.87	...	3.21
A3571	0.040	$6.9 \pm 0.3$	$6.9 \pm 0.2$	1.97	1.83	4.36	10.78
A3667	0.053	$7.0 \pm 0.6$	$7.0 \pm 0.6$	2.18	2.22	5.34	7.36
A4059	0.048	$4.1 \pm 0.3$	$4.4 \pm 0.3$	0.81	0.66	1.22	2.67
Cyg A*	0.057	$6.5 \pm 0.6$	$6.1 \pm 0.4$	2.70	2.01	4.46	5.79
MKW3S	0.045	$3.5 \pm 0.2$	$3.7 \pm 0.2$	0.75	0.54	0.91	2.47
Triang*	0.051	$9.5 \pm 0.7$	$9.6 \pm 0.6$	3.12	3.13	9.13	11.21

NOTES: Temperatures are in keV; luminosities are in units of  $10^{44} h^{-2} \text{ erg s}^{-1}$ ; fluxes are corrected for absorption and in units of  $10^{-11} \text{ erg s}^{-1} \text{ cm}^{-2}$ . Subscript X denotes 0.1–2.4 keV energy band; bol is for bolometric. Clusters with \* are at  $|b| < 20^\circ$  and the flux of the cluster with † is below the limit; these clusters are used for the  $L_X - T$  relation only.

<sup>a</sup> Single-temperature fits and cooling flow-corrected emission-weighted temperatures with 90% errors are from M98, except those marked d which are from David et al. (1993) and e which are estimated from the  $L_X - T$  relation derived here.

<sup>b</sup> Total luminosities within  $r < 1 h^{-1} \text{ Mpc}$  (including cooling flow regions).

<sup>c</sup> Corrected quantities (cooling flow regions excised).

For all clusters in the sample except 4, *ASCA* wide-beam as well as emission-weighted cooling flow-excluded temperatures are derived in M98 and references therein. These temperatures correspond to averaging over  $r = 0.6 - 1 h^{-1} \text{ Mpc}$  apertures, dependent on the individual observation details; because the total cluster emission is dominated by bright central regions, such a difference in radial coverage is unimportant. For the remaining 4 clusters without the *ASCA* data, temperatures are estimated from the  $L_X - T$  relation derived in §. Non-*ASCA* wide-beam temperatures for these clusters exist (David et al. 1993) and

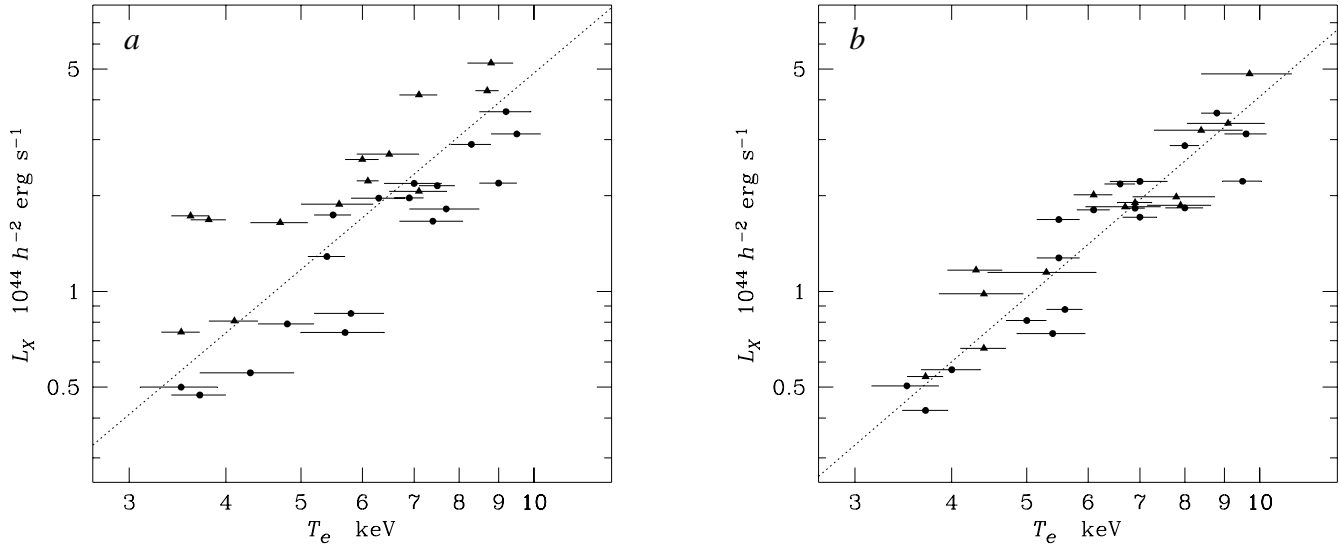


FIG. 1.—Luminosities in the 0.1–2.4 keV band vs. temperatures from Table 1. Panel (a) shows total luminosities within  $r = 1 h^{-1}$  Mpc and single-temperature fits to the overall *ASCA* spectra, while panel (b) shows corrected luminosities with cooling flow regions excised (see text) vs. emission-weighted temperatures derived from the temperature maps excluding cooling flow components. Triangles mark clusters with strong cooling flows, circles are clusters with weak or no cooling flows. Dashed lines are respective best-fit power laws from Table 2.

are consistent, within their relatively large uncertainties, with the estimated values. We will use our estimates for the temperature function, since those measured temperatures are not cooling flow-corrected. For clusters with *ASCA* temperatures, Table 1 also lists cooling flow-excised bolometric luminosities, estimated from the corrected 0.1–2.4 keV luminosities using the corrected temperature and assuming isothermality. Our redshift interval, imposed by the *ASCA* analysis constraints (see M98), effectively excludes clusters with  $T \lesssim 3.5$  keV.

For the temperature function determination, as opposed to the  $L_X - T$  relation, completeness of the sample is important. Therefore, as in previous analyses, the  $|b| < 20^\circ$  area is excluded from the temperature function subsample. Ebeling et al. (1996) find that their originally optically selected list is already noticeably incomplete in the interval  $20^\circ < |b| < 30^\circ$ . Excluding this area does not change our results, so this small effect is ignored. Note that our sample, which consists of bright, moderately nearby clusters with a flux limit a factor of 4 above the completeness limit of the Ebeling et al. (1996) list, is less likely to be affected by the above effect than their full list. In §, we confirm the completeness of our sample using the luminosity function from the purely X-ray selected RASS cluster catalog (Ebeling et al. 1997; the catalog itself is unavailable at the time of this writing).

The subsample of 30 clusters used for the temperature function has a median temperature and redshift of about 6 keV and 0.054, respectively. It overlaps to a large degree the samples of E90 and HA, both selected by 2–10 keV flux, but differs from them mainly at low temperatures and fluxes. Unlike our sample, the E90 dataset is not limited by redshift, which improves statistics by including several hot, distant clusters, but has the disadvantage of complicating the evolutionary studies. Our sample has a lower effective flux limit than HA and therefore has more clusters in the corresponding temperature range. The main improvement upon previous datasets is, of course, the higher-quality imaging and temperature data, including spatially resolved temperature measurements, available to us.

### 3. THE $L_X - T$ RELATION

Table 1 shows that for strong cooling flow clusters, the cooling flow-corrected temperatures are significantly higher than the wide-beam values, and that the small central regions contain a significant fraction of the total X-ray luminosity. Below the luminosity-temperature relation in its traditional meaning, using wide-beam temperatures and total luminosities, is compared to the one that corresponds only to the main cluster gas, excluding cooling flows in clusters that have ones.

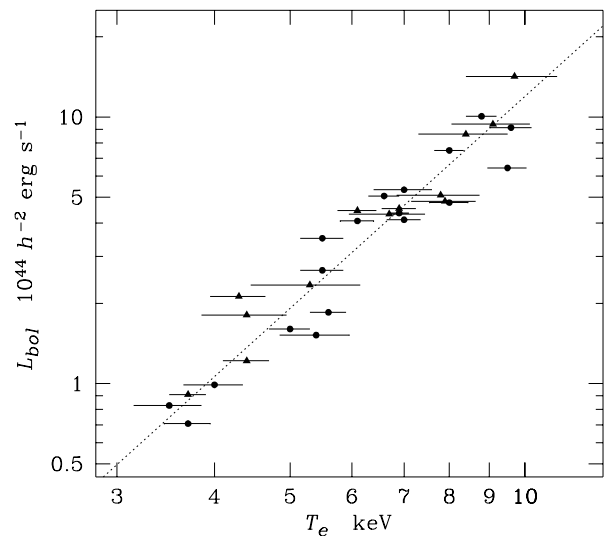


FIG. 2.—Same as Fig. 1b (luminosities vs. temperatures both corrected for cooling flows) but for bolometric luminosities.

Figure 1 shows luminosities in the 0.1–2.4 keV band vs. temperatures for clusters with *ASCA* data, including and excluding the cooling flow regions. Corrected bolometric luminosities vs. corrected temperatures are plotted in Fig. 2. These  $L - T$  relations are fit by power laws of the form  $L = A_6 T_6^\alpha$ , where

$T_6 \equiv T/6$  keV, using the bisector modification of the Akritas & Bershadsky (1996 and references therein) linear regression algorithm that allows for intrinsic scatter and nonuniform measurement errors and treats  $L$  and  $T$  symmetrically. The confidence intervals are evaluated by bootstrap resampling (e.g., Press et al. 1992) while simultaneously adding random measurement errors to the temperatures and 5% errors to the luminosities (the results do not depend on the latter). Table 2 lists the best-fit parameters together with the residual rms scatter in  $\log L$  for a given  $T$ ,  $\sigma_{\log L}$  (the scatter along the  $T$  axis is  $\sigma_{\log T} \simeq \sigma_{\log L}/\alpha$ ). We also include a fit for the cooling flow-corrected temperatures vs. total luminosities, which may be useful, for example, to relate theoretical predictions to the fluxes of poorly resolved distant clusters. Note that the 0.1–2.4 keV gas emissivity is only weakly dependent on temperature in the considered temperature range, so the slope  $\alpha$  of the  $L_{\text{bol}} - T$  relation should be greater than that for the 0.1–2.4 keV band by about 0.5 without any corrections.

TABLE 2  
FITS TO  $L - T$  RELATIONS

Band keV	Data	$A_6$ $10^{44} h^{-2} \text{ erg s}^{-1}$	$\alpha$	$\sigma_{\log L}$
0.1–2.4	Uncorr. $T$ , total $L$	$1.71 \pm 0.21$	$2.02 \pm 0.40$	0.181
0.1–2.4	Corr. $T$ , total $L$	$1.57 \pm 0.17$	$2.09 \pm 0.29$	0.133
0.1–2.4	Corr. $T$ , corr. $L$	$1.41 \pm 0.12$	$2.10 \pm 0.24$	0.104
Bol.	Corr. $T$ , corr. $L$	$3.11 \pm 0.27$	$2.64 \pm 0.27$	0.103

Figure 1 and Table 2 show that the scatter in the  $L_X - T$  relation is greatly reduced when cooling flows are excised and the quantities representing only the main cluster gas are compared. An example of the two largest deviations around 3.7 keV in Fig. 1a, which are A780 (Hydra A) and A2597, shows that the improvement is due in equal degrees to the corrections of the temperature and luminosity. The same can be seen in the last column of Table 2. Such a strong effect of the cooling flows on the wide-beam temperatures was not anticipated before ASCA, and the cooling flow luminosity alone is insufficient to account for the scatter. This led Fabian et al. (1994) to suggest that cooling flow clusters are different from others in their global gas properties. Our results show that most of the scatter in the  $L_X - T$  relation is due to localized,  $r \lesssim 50 h^{-1}$  kpc regions with cooling flows. On the other hand, after the exclusion of these regions, some residual scatter remains, which indeed is likely to be due to the different gas distributions — after the corrections, the largest deviation at 9.5 keV in Fig. 1b is a strong merger A754. Note that a small fraction of the scatter is due to the temperature measurement errors.

The derived  $L_X - T$  relation and its intrinsic scatter can be compared to theoretical and numerical predictions that at present do not model radiative cooling adequately. A self-similar model of cluster growth (Kaiser 1986), supported by simulations that include only gravity (e.g., Navarro et al. 1995), predicts  $L_{\text{bol}} \propto T^2$ . A disagreement of this prediction and the observed steeper slope has long been noted; our new  $L_{\text{bol}} - T$  relation is also significantly steeper. To explain this disagreement, it was proposed that hypothetical preheating of the intracluster gas, e.g., by supernovae, effectively reduces the central gas densities with a stronger effect on the cooler clusters (e.g., Kaiser 1991; Evrard & Henry 1991; Navarro et al. 1995; Cavaliere et al. 1997). Assuming that, after initial preheating, gas in the cluster cores remains on the same adiabat as clusters evolve, Evrard & Henry predict a scale-free relation  $L_{\text{bol}} \propto T^{2.75}$ . How-

ever, cluster merging should result in significant increase of the gas specific entropy due to shock-heating, as is indeed observed (e.g., Markevitch et al. 1998b). Cavaliere et al. allow the gas inside the cores to be shock-heated and mixed in addition to an early injection of the energy equivalent to 0.5–0.8 keV per gas particle. Their predicted  $L_{\text{bol}} - T$  slope changes from 5 on the group scale to 2 on the hottest cluster scale, being  $\sim 2.3$  in the temperature interval covered by our data. They also predict a scatter in the  $L_{\text{bol}} - T$  relation of about  $\sigma_{\log L} \simeq 0.13$  due to the differing merging histories of individual clusters. Considering the number of adjustable quantities in such modeling, these predictions are quite close to our observations. Although our data are adequately described by a single power law, with such a small scatter it is quite feasible to measure the predicted steepening of the  $L - T$  slope toward lower temperatures, if comparably accurate data at those temperatures are obtained. Such a measurement would provide interesting information on the energetics of the intracluster gas.

The observed tight  $L_X - T$  correlation has other implications. M. Arnaud (1997, private communication) used the small scatter of  $L_X$  for clusters lacking cooling flows to constrain the cluster-to-cluster baryon fraction variations. We also note for illustration that our scatter in low-redshift  $L_X$  is equivalent to  $0.25^m$ , which is comparable to  $\sim 0.19^m$  for Type Ia supernovae used for cosmological distance estimates (Perlmutter et al. 1997). However, clusters are not expected to remain standard candles at all redshifts.

After this paper has been submitted for publication, we received a preprint by Allen & Fabian (1998) who employed a different approach to evaluate the effect of cooling flows on the  $L_X - T$  relation for hot clusters. They modeled the overall cluster spectra by a sum of the isothermal and cooling flow components and took the temperature of the isothermal component as the true average cluster temperature. This compares to the M98 approach of using spatially resolved spectra to localize cooling flow regions, obtain temperature maps outside these regions, and use these maps to calculate average temperatures. Allen & Fabian find generally similar temperature bias for those clusters studied in both works, although the exact temperature values are sometimes different due to the difference in approach. Unlike our result, the Allen & Fabian’s corrected  $L_X - T$  relation still has considerable scatter and shows difference between clusters with and without cooling flows. This is because their luminosities include cooling flow regions, while we excise these regions when calculating the corrected luminosities. Nevertheless, the slope of the corrected  $L_{\text{bol}} \propto T^\alpha$  relation obtained by Allen & Fabian,  $\alpha = 2.3_{-0.3}^{+0.6}$ , is in good agreement with our result.

## 4. THE TEMPERATURE FUNCTION

### 4.1. Derivation

The temperature function (TF), which is the number of clusters per unit comoving volume and unit temperature interval,  $dN/dT$ , or the number above a given temperature,  $N(> T)$ , can be derived by co-adding all clusters with weights  $1/V(T)$ . Here  $V(T)$  is the maximum comoving volume within which a cluster with a given temperature could have been detected above the flux limit of our sample, and  $T$  is a cooling flow-corrected temperature. Since the sample is flux-limited rather than temperature-limited, an  $L_X - T$  relation has to be used to calculate the volume as a function of temperature. The sample was selected using the fluxes with excised cooling flows and we

can take advantage of the tight  $L_X - T$  relation obtained above. The volume as a function of temperature was calculated by integrating, over the redshift interval 0.04–0.09, volume elements with weights equal to the probability of a cluster with a given temperature to have a detectable flux, assuming a log-Gaussian scatter in the  $L_X - T$  relation given in Table 2. For a purely flux-limited sample, a symmetric  $L_X - T$  scatter such as that results in a uniform increase of the volume by a factor of about 1.06, compared to no scatter.<sup>2</sup> In the presence of the redshift constraints, the scatter results in the volume correction between a factor of 1.26 at our minimum  $T = 3.5$  keV and 0.88 at 6.5 keV. The sample is essentially volume-limited above  $\sim 7$  keV.

Note that this approach to the derivation of the TF differs from the one employed, e.g., in HA and other works, in which individual cluster luminosities (rather than temperatures) are used to determine the volume within which a given cluster would have a detectable flux. The latter method is entirely appropriate for the derivation of a luminosity function, but it is not optimal for the TF, because clusters with a given temperature have a wide range of luminosities. This method does result in an unbiased, on average, TF estimate in the limit of the large number of clusters. In reality, however, the number of clusters is always limited, and the large intrinsic scatter in the  $L_X - T$  relation causes bias in the median and most probable TF estimates, especially at the highest (lowest) temperatures where the TF is estimated using only one or two hottest (coolest) clusters in the sample. To quantify this bias for a purely flux-limited sample, we performed a simple simulation, scattering randomly in Euclidean space clusters with luminosities distributed with an rms Gaussian scatter in  $\log L_X$  of 0.28 (which corresponds to the  $L_X - T$  scatter in HA). For those simulated clusters above the flux limit, search volumes were calculated using individual luminosities,  $V \propto L^{3/2}$ . The resulting distribution of the calculated weights  $1/V$  is strongly skewed; the median derived TF is only 0.65 of the average (true) value at a temperature of the single hottest cluster in the sample, while the most probable TF value is only 0.32 of the average. The reason is that for any temperature, there are many more overluminous clusters in a flux-limited sample than underluminous ones (for the adopted value of the  $L_X - T$  scatter, the ratio is 5:1).<sup>3</sup> The TF derivation method employed in this paper is free of this small-number bias. Its possible disadvantage is the reliance on the validity of the  $L_X - T$  relation at all temperatures, including the extreme ones where the number of clusters in the  $L_X - T$  sample is small. However, this does not apply to our sample, since it is volume-limited above  $\sim 7$  keV, which means the search volume for hot clusters is simply the total volume between  $0.04 < z < 0.09$ .

The uncertainty of the resulting temperature function is evaluated by bootstrap resampling, assuming a Poissonian distribution of the total number of clusters in the sample and adding random Gaussian measurement errors to the individual temperatures at each resampling. The latter is a minor contribution to the overall uncertainty dominated by that of the small number of clusters.

The resulting cumulative temperature function is plotted in Fig. 3, overlaid in panel (a) on the previously derived functions of E90 and HA (the latter is taken from Eke et al. 1996). The figure shows that the overall effect of our corrections for the presence of cooling flows at each stage of the derivation is not

large — there is agreement with the earlier E90 and HA functions within their  $1\sigma$  uncertainties (not shown). The cooling flow correction on average results in a small shift of the TF toward higher temperatures. An apparent (not highly significant) disagreement between our and HA results at high temperatures is mostly due to (a) the fact that our sample is volume-limited while the HA sample is flux-limited, (b) a possible incompleteness of the HA sample (e.g., it does not include the hot cluster A2163 which appears to satisfy the selection criteria), and (c) the possibility of the small-number bias described above.

To assess the completeness of our sample, particularly at low temperatures where the Abell catalog may miss objects even at high Galactic latitudes (e.g., MKW3S), we use the luminosity function obtained from the purely X-ray selected RASS cluster catalog (Ebeling et al. 1997) and convert it into the temperature function using the  $L_X - T$  relation and its scatter. The relevant  $L_X - T$  relation was derived using the total, RASS-measured (Ebeling et al. 1996) luminosities and corrected temperatures of our clusters. The resulting relation is similar to line 2 in Table 2 but has a larger scatter due to the RASS flux uncertainties. The resulting temperature function, shown in Fig. 3a, is in excellent agreement with our result, indicating that no significant number of cool clusters is missing. The luminosity function was derived from a much larger cluster sample than ours so its uncertainty is negligible.

To obtain an analytic fit to the differential temperature function, we use fine temperature binning and maximum likelihood minimization assuming a Poissonian distribution of the cluster number in each bin (bins are allowed to have zero clusters; the results are independent of the bin size). The errors are calculated by the bootstrap algorithm outlined above. For a power law of the form  $dN/dT = A_6 T_6^{-\alpha}$ , we obtain, assuming  $\Omega_0 = 1$ ,  $A_6 = 1.90 \pm 0.54 \times 10^{-7} h^3 \text{Mpc}^{-3} \text{keV}^{-1}$  and  $\alpha = 4.2 \pm 0.7$ . A slightly better fit is obtained for an exponential  $A_6 \exp[-(T - 6 \text{ keV})/T_*]$  with  $A_6 = 2.38 \pm 0.68 \times 10^{-7} h^3 \text{Mpc}^{-3} \text{keV}^{-1}$  and  $T_* = 1.6 \pm 0.4$  keV. These models are shown in cumulative form in Fig. 3b.

#### 4.2. Constraining the Fluctuation Spectrum

The cluster temperature function was used to obtain constraints on the cosmological density fluctuation spectrum by many authors (the incomplete listing includes HA; Kaiser 1991; White, Efstathiou, & Frenk 1993; Viana & Liddle 1996; Eke et al. 1996; Colafrancesco, Mazzotta, & Vittorio 1997; Pen 1998) applying the Press & Schechter (1974) formalism supplemented by simulations. Our temperature function is slightly higher and flatter than the previous estimates, and its accuracy is better. In addition, Markevitch & Vikhlinin (1997) and M98 recently showed that the observed cluster nonisothermality considerably reduces the X-ray mass estimate for a given emission-weighted temperature, compared to the previously made estimates. An accurate comparison of cosmological models to the data requires hydrodynamic simulations to take into account the nonequilibrium state of many clusters. However, we can perform a qualitative estimate of the effect of the above observational updates on the fluctuation spectrum constraints by applying the Press-Schechter formalism for  $\Omega_0 = 1$  and  $\Omega_0 = 0.3$  ( $\Lambda = 0$ ), and comparing the results to similar previous analyses.

<sup>2</sup>The reason is geometric; the redshift shell  $[z, z + \Delta z]$  containing the overluminous clusters has greater volume than the shell  $[z - \Delta z, z]$  containing the underluminous ones.

<sup>3</sup>In principle, this may also affect the validity of the  $L_X - T$  relation derived from a flux-limited sample. However, for our sample, selected by the corrected fluxes and with a much smaller scatter in the corrected  $L_X - T$  relation, this effect is small.

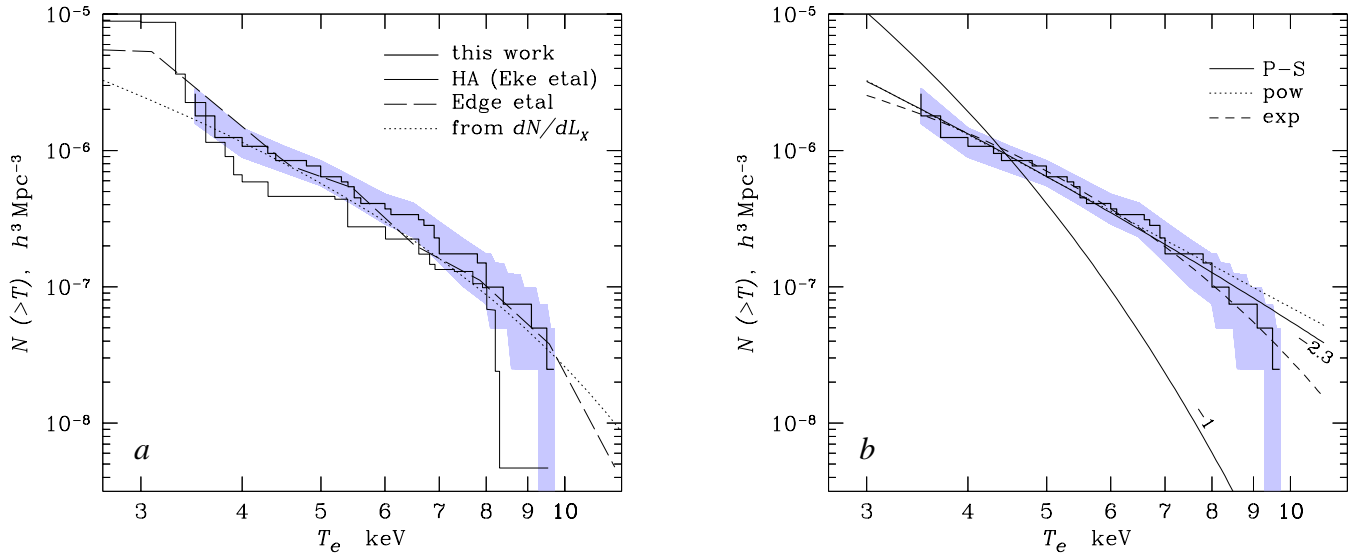


FIG. 3.—Cumulative temperature function. Panel (a) shows our result (assuming  $\Omega_0 = 1$ ) with its 68% error band overlaid on the earlier derivations of HA and E90, as well as a function obtained from the luminosity function for a purely X-ray selected sample (Ebeling et al. 1997) using the  $L_X - T$  relation (see text). Panel (b) shows fits to our data: Press-Schechter fits for  $n = -1$  (standard CDM) and  $n = -2.3$  (best-fit for  $\Omega_0 = 1$ ), and empirical power law and exponential fits (see text).

A full description of the formalism can be found in the references above, so only the relevant definitions are given here.

We assume that the power spectrum of linear density fluctuations on the cluster scale is  $P_k \propto k^n$ , implying an rms amplitude of the linear mass fluctuations in a sphere containing an average mass  $M$  of  $\sigma(M) = \sigma_8 (M/m_8)^{-(n+3)/6} (1+z)^{-1}$ , where  $m_8$  is the average mass within the comoving  $r = 8h^{-1}$  Mpc. Our clusters are assumed to lie at the median sample redshift of 0.054, being observed just after their collapse (a reasonable assumption for  $\Omega_0 = 1$  but not necessarily such for  $\Omega_0 \ll 1$ , e.g., White & Rees 1978; nevertheless, we use this assumption for  $\Omega_0 = 0.3$  for comparison with other works). The cluster mass within a radius of overdensity  $\Delta_c$  (taking  $\Delta_c = 178$  for  $\Omega_0 = 1$  and  $\Delta_c = 124$  for  $\Omega_0 = 0.3$  as in Eke et al. 1996), is assumed to scale with the X-ray emission-weighted temperature as  $M = M_{10}(T/10 \text{ keV})^{3/2}$  with an rms scatter of 20% as predicted by simulations of Evrard, Metzler, & Navarro (1996).

It is worth mentioning here that the scaling  $M \propto T^{3/2}$  follows from the same line of argument as the relation  $L_{\text{bol}} \propto T^2$ , and the latter is not observed. Processes that modify the  $L_X - T$  relation, e.g., preheating, can possibly break the  $M - T$  scaling. However, X-ray luminosity is very sensitive to the gas density distribution, which is more likely to change due to preheating than the gas temperature. Indeed, simulations by Metzler & Evrard (1998) suggest that the  $M - T$  relation holds at least for their considered preheating model, while the gas density distributions (and therefore the  $L_X - T$  relation) are significantly modified. The available observational data (masses from gravitational lensing vs. X-ray temperatures) at least do not contradict the adopted  $M - T$  relation (Hjorth, Oukbir, & van Kampen 1998). X-ray measurements of masses at different temperatures (our work in progress) will further test the accuracy of this scaling.

For  $M_{10}$  we use two values for each assumed  $\Omega_0$  (values in parentheses correspond to  $\Omega_0 = 0.3$ ),  $13.5 (16.4) \times 10^{14} h^{-1} M_\odot$  which assumes cluster isothermality (e.g., Eke et al. 1996) and  $9.1 (9.8) \times 10^{14} h^{-1} M_\odot$  which corresponds to the mass pro-

file of the main cluster of A2256 derived by Markevitch & Vikhlinin using the observed temperature profile. Although the latter values are based on a single cluster, temperature profiles for many other clusters are similar and the effect on the mass is expected to be similar as well (M98). Using these relations,  $m_8 = 6 \times 10^{14} \Omega_0 h^{-1} M_\odot$  corresponds to  $T \simeq 3 - 8 \text{ keV}$  for  $\Omega_0 = 0.3 - 1$ , indicating that the cluster data best constrain the density fluctuations at this particular scale.

The Press-Schechter mass function was converted to the differential temperature function which was then fitted to the data as described in §, with  $\sigma_8$  and  $n$  being free parameters. The observed TF was derived self-consistently using the two values of  $\Omega_0$ . The best-fit  $\sigma_8$  and  $n$  are given in Table 3 for the two cosmologies and two assumed cluster temperature distributions. The best-fit model TF in the cumulative form for  $\Omega_0 = 1$  is shown in Fig. 3b (the two temperature profile cases are almost identical). As was noted in previous works, because the abundance of clusters is very sensitive to  $\sigma_8$ , the latter quantity is rather robust to the uncertainty in the number of clusters. Therefore, even though our temperature function is about a factor of 2 above that of HA used in most previous works, our  $\sigma_8$  for the isothermal case and  $\Omega_0 = 1$  is only slightly higher than the values derived from the corrected HA data (0.50, Eke et al. 1996, 1998; 0.53, Pen 1998). Our result for  $\Omega_0 = 0.3$  is significantly different from the above two works which report  $\sigma_8 \simeq 0.9$  for  $\Omega_0 = 0.3$ . The difference is due to our treatment of  $n$  as a free parameter; fixing  $n \simeq -1.3$  or  $-1.4$  as in those works and assuming isothermality results in best-fit  $\sigma_8$  values close to those in the above works, for both values of  $\Omega_0$ . However, such values of  $n$  do not fit the data.

TABLE 3  
PRESS-SCHECHTER FITS TO THE TEMPERATURE FUNCTION

T PROFILE	$\Omega_0 = 1$		$\Omega_0 = 0.3$	
	$\sigma_8$	$n$	$\sigma_8$	$n$
ISOTHERMAL	$0.55 \pm 0.03$	$-2.3 \pm 0.3$	$0.78 \pm 0.04$	$-2.0 \pm 0.3$
OBSERVED	$0.51 \pm 0.03$	$-2.3 \pm 0.3$	$0.66 \pm 0.03$	$-2.1 \pm 0.3$

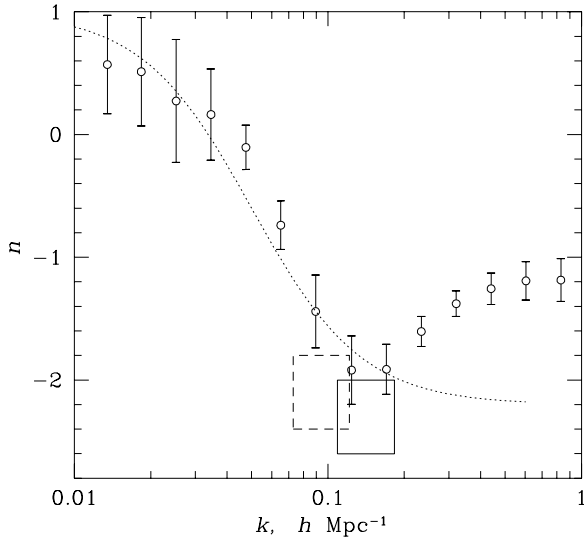


FIG. 4.—Circles with  $1\sigma$  errors show the slope of the APM galaxy density fluctuation spectrum ( $P_k \propto k^n$ ) as a function of scale, from Baugh & Gaztañaga (1996). Flattening of the observed spectrum at  $k \gtrsim 0.2$  reflects the onset of nonlinear fluctuation growth; dotted line is a fit to the de-evolved, linear spectrum. Rectangles show our slope of the linear spectrum (solid line for  $\Omega_0 = 1$ , dashed line for  $\Omega_0 = 0.3$ ). Their vertical sizes are the 90% errors, while their horizontal sizes illustrate the approximate  $k$  coverage corresponding to our temperature range. The rectangles are plotted at  $k = 1/r$ , where  $r$  is the radius containing the average mass  $M$  corresponding to a given temperature. A more meaningful average  $k$  weighted by the contribution of each harmonic to  $\sigma(M)$  depends on the exact spectrum, so the rectangle positions are rather approximate.

The derived  $\sigma_8$  is sensitive to the assumed mass-temperature relation. The observed nonisothermality, which modifies this relation, acts to reduce the derived value (see Table 3); the scatter in the relation, included in all our estimates, also reduces the  $\sigma_8$  estimate by  $\sim 0.01$ . Since some of the observed radial temperature decline may be due to the incomplete thermalization of the gas in the outermost cluster regions (biasing low the X-ray-derived total mass), detailed cluster simulations reproducing such a decline are necessary for an accurate interpretation of the temperature function. In the absence of such simulations, the  $\sigma_8$  values obtained above may be viewed as conservative brackets of the true value for the assumed cosmologies.

The best-fit fluctuation spectrum slope is  $n = -2.3$  and  $n \simeq -2$  for  $\Omega_0 = 1$  and  $\Omega_0 = 0.3$ , respectively; the results are very close for isothermal and nonisothermal cases (see Table 3). The value corresponding to  $\Omega_0 = 1$  is consistent with  $n \simeq -2$  obtained by Kaiser (1991) using the E90 data and is marginally steeper than  $n = -(1.7^{+0.65}_{-0.35})$  (68% two-parameter interval) reported by HA and  $n = -1.8 \pm 0.4$  by Colafrancesco et al. (1997) using the HA data. Our weak dependence of the best-fit  $n$  values on  $\Omega_0$  seems to disagree with the Colafrancesco et al. finding; however, it is difficult to compare fits to the TFs with rather different observed shapes.

Our temperature interval corresponds to the log range in the wavenumber  $k$  of only 0.23 (although a comparable interval of  $k$  contributes to the mass fluctuation  $\sigma(M)$  at any  $M$ ), thus it probes a local shape of the fluctuation spectrum. Coincidentally, the galaxy fluctuation spectrum derived from the APM survey, which is the most accurate determination to date (Baugh & Efstathiou 1993 and references therein; Baugh & Gaztañaga

1996), exhibits maximum steepness at this scale with a local slope of  $n \simeq -1.9 \pm 0.3$  (68% interval). Figure 4 shows the observed APM slope as a function of scale from Baugh & Gaztañaga together with our measurement. Flattening at  $k \gtrsim 0.2$  reflects the onset of nonlinear fluctuation growth; the above authors recover the approximate primordial, linear spectrum (dotted line in Fig. 4) with  $n \simeq -2$  on these scales. The reconstructed linear-regime slope as well as the observed slope are in agreement with our X-ray results. It is worth recalling that the galaxy distribution is linked to the underlying, almost linear, density field via an unknown and possibly scale-dependent bias. Clusters, on the other hand, represent nonlinearly evolved density peaks and their abundance constrains the density spectrum directly, under the assumption of gaussianity of the fluctuations (and, of course, assuming that the X-ray-measured cluster masses are not grossly in error). Agreement between two such widely different methods is encouraging. Both the optical and the X-ray slope are considerably steeper than the standard CDM prediction of  $n \simeq -1$  at this scale (e.g., Blumenthal et al. 1984). For illustration of the discrepancy with the X-ray data, Fig. 3b shows a temperature function for  $n = -1$ . A discussion of some promising alternatives (namely, mixed dark matter) can be found, e.g., in Baugh & Efstathiou (1993).

## 5. SUMMARY AND FUTURE WORK

Using the new *ASCA* cluster temperatures and *ROSAT* luminosities, both calculated directly excluding the cooling flow regions, we obtain the  $L_X - T$  relation in the 3.5–10 keV temperature interval with greatly reduced scatter. This result provides an accurate reference point (a) for a comparison with nearby, cooler clusters and groups that should have a different slope if there was preheating, and (b) for evolution studies using the oncoming *AXAF* data which will provide the necessary angular resolution for cooling flow excision at higher redshifts. The derived  $L_X - T$  relation can be directly compared to theoretical and numerical predictions, most of which do not include a detailed treatment of radiative cooling.

These new data are also used to rederive the nearby cluster temperature function. This function is interpreted qualitatively by applying the Press-Schechter formalism for  $\Omega_0 = 1$  and  $\Omega_0 = 0.3$ , to obtain values of  $\sigma_8$  assuming the isothermal and observed cluster temperature profiles (see Table 3). These values should bracket the correct value if some of the observed radial temperature decline in clusters is due to the incomplete thermalization of the gas in the outer regions. The derived slope of the mass fluctuation spectrum at the cluster scale is  $n = -(2.0 - 2.3) \pm 0.3$  for considered values of  $\Omega_0$ , which is consistent with the APM galaxy survey at the same scale. Again, our temperature function provides a reference for future accurate evolution studies and for direct comparison with theoretical predictions.

It would be interesting to extend the temperature range of this work to lower temperatures, 1–3 keV, where one expects to see, for example, the effects of preheating on the  $L_X - T$  relation. It would also greatly strengthen the constraints from the temperature function. Such an extension will be possible when X-ray selected cluster catalogs become available. Since preheating can modify the simple mass-temperature scaling, accurate measurements of cluster masses over a range of temperatures, including the lowest, will be required for the interpretation of such an extended temperature function.

The author is grateful to Alexey Vikhlinin, Bill Forman and Vincent Eke for useful discussions and comments. The results reported here would not be possible without the dedicated work of the *ASCA* and *ROSAT* teams on building, calibration and op-

eration of the instruments. The HEASARC online data archive at NASA/GSFC has been used extensively in this research. The work was supported by NASA contract NAS8-39073.

## REFERENCES

- Akritas, M. G., & Bershad, M. A. 1996, *ApJ*, 470, 706  
 Allen, S. W. 1998, *MNRAS*, submitted; astro-ph/9710217  
 Allen, S. W., & Fabian, A. C. 1998, *MNRAS*, submitted; astro-ph/9802218  
 Baugh, C. M., & Gaztañaga, E. 1996, *MNRAS*, 280, L37  
 Baugh, C. M., & Efstathiou, G. 1993, *MNRAS*, 265, 145  
 Blumenthal, G. R., Faber, S. M., Primack, J. R., & Rees, M. J. 1984, *Nature*, 311, 517  
 Cavaliere, A., Menci, N., & Tozzi, P. 1997, *ApJ*, 484, L21  
 Colafrancesco, S., Mazzotta, P., Vittorio, N. 1997, *ApJ*, 488, 566  
 David, L., Forman, W., & Jones, C. 1991, *ApJ*, 380, 39  
 David, L., Slyz, A., Jones, C., Forman, W., Vrtilik, S. D., & Arnaud, K. A. 1993, *ApJ*, 412, 479  
 Ebeling, H., Voges, W., Böhringer, H., Edge, A. C., Huchra, J. P., & Briel, U. G. 1996, *MNRAS*, 281, 799  
 Ebeling, H., Edge, A. C., Fabian, A. C., Allen, S. W., Crawford, C. S., & Böhringer, H. 1997, *ApJ*, 479, L101  
 Edge, A. C., & Stewart, G. C. 1991, *MNRAS*, 252, 414  
 Edge, A. C., & Stewart, G. C., Fabian, A. C. 1992, *MNRAS*, 258, 177  
 Edge, A. C., Stewart, G. C., Fabian, A. C., & Arnaud, K. A. 1990, *MNRAS*, 245, 559 (E90)  
 Eke, V. R., Cole, S., & Frenk, C. S. 1996, *MNRAS*, 282, 263  
 Eke, V. R., Cole, S., & Frenk, C. S., Henry, J. P. 1998, *MNRAS*, submitted; astro-ph/9802350  
 Eke, V. R., Navarro, J. F., & Frenk, C. S. 1998, *ApJ*, submitted; astro-ph/9708070  
 Evrard, A. E., & Henry, J. P. 1991, *ApJ*, 383, 95  
 Evrard, A. E., Metzler, C. A., & Navarro, J. F. 1996, *ApJ*, 469, 494  
 Fabian, A. C., Crawford, C. S., Edge, A. C., & Mushotzky, R. F. 1994, *MNRAS*, 267, 779  
 Fukazawa, Y. 1997, PhD thesis, University of Tokyo  
 Henry, J. P. 1997, *ApJ*, 489, L1  
 Henry, J. P., & Arnaud, K. A. 1991, 372, 410 (HA)  
 Hjorth, J., Oukbir, J., van Kampen, E. 1998, *MNRAS*, in press; astro-ph/9802293  
 Jones, C., & Forman, W. 1984, *ApJ*, 276, 38  
 Kaiser, N. 1986, *MNRAS*, 222, 323  
 Kaiser, N. 1991, *ApJ*, 383, 104  
 Loewenstein, M., & Mushotzky, R. F. 1996, *ApJ*, 466, 695  
 Markevitch, M., Forman, W. R., Sarazin, C. L., & Vikhlinin, A. 1998a, *ApJ*, in press; astro-ph/9711289 (M98)  
 Markevitch, M., et al. 1998b, in preparation  
 Markevitch, M., & Vikhlinin, A. 1997, *ApJ*, 491, 467  
 Metzler, C. A., & Evrard, A. E. 1998, *ApJ*, submitted; astro-ph/9710324  
 Mushotzky, R. F. 1984, *Phys. Scripta*, T7, 157  
 Mushotzky, R. F., Scharf, C. A. 1997, *ApJ*, 482, L13  
 Navarro, J. F., Frenk, C. S., & White, S. D. M. 1995, *MNRAS*, 275, 720  
 Pen, U. 1998, *ApJ*, in press; astro-ph/9610147  
 Perlmutter, S., et al. 1997, *ApJ*, 483, 565  
 Ponman, T. L., Bourner, P. D. J., Ebeling, H., & Böhringer, H. 1996, *MNRAS*, 283, 690  
 Press, W. H., & Schechter, P. L. 1974, *ApJ*, 187, 425  
 Press, W. H., Teukolsky, S. A., Vetterling, W. T., & Flannery, B. P. 1992, *Numerical Recipes* (Cambridge University Press)  
 Tsuru, T., Koyama, K., Hughes, J., Arimoto, N., Kii, T., & Hattori, M. 1996, "UV and X-ray Spectroscopy of Astrophysical Plasmas", ed. K. Yamashita (Tokyo: Universal Academy), 375  
 Viana, P. T. P., & Liddle, A. R. 1996, *MNRAS*, 281, 323  
 White, S. D. M., Efstathiou, G., & Frenk, C. S. 1993, *MNRAS*, 262, 1023  
 White, S. D. M., & Rees, M. J. 1978, *MNRAS*, 183, 341